

Atomic scale evidence for faceting stabilization of a polar oxide surface

Frank Ostendorf, Stefan Torbrügge, and Michael Reichling*

Fachbereich Physik, Universität Osnabrück, BarbarasträÙe 7, 49076 Osnabrück, Germany

(Received 12 November 2007; published 9 January 2008)

By highest-resolution dynamic scanning force microscopy operated in the non-contact mode, we reveal the complex stabilization mechanism of polar zinc-terminated ZnO(0001). The nanoscopic and atomic structures unveiled corroborate a model of stabilization via triangular structures. High-temperature preparation ($T > 1300$ K) yields a phase with an additional stabilization by faceting in the form of highly ordered step arrays. The terraces between steps are partly covered with triangular reconstructions exhibiting exclusively $\{10\bar{1}0\}$ nanofacets on step edges. Both mechanisms together allow a complete stabilization of the surface without the involvement of adsorbates.

DOI: [10.1103/PhysRevB.77.041405](https://doi.org/10.1103/PhysRevB.77.041405)

PACS number(s): 68.47.Gh, 68.35.B-, 68.37.Ps, 82.65.+r

Polar oxide surfaces play a key role in a variety of technologies like catalysis¹ or gas sensing systems.² For the development and improvement of the efficiency of functional oxide materials,³ for instance, used in methanol or water-gas shift catalysis,⁴ a detailed understanding of surface structure and morphology is important. Moreover, polarity is a general phenomenon that may be found on the surface of any ionic crystal exhibiting an alternating stacking of oppositely charged ionic planes parallel to the surface. If the resulting dipole moment perpendicular to the surface is nonzero, a simple termination of the bulk structure is not possible. The stabilization of such a “Tasker type 3” surface⁵ can be accomplished by a rearrangement of surface charges or by the introduction of compensation charges into the outer surface planes.⁵⁻⁷ This involves a significant modification of the surface geometric and electronic structure and a major change in surface stoichiometry.

One of the most prominent examples of a polar metal oxide surface is zinc oxide (ZnO). ZnO crystallizes in the hexagonal wurtzite structure, revealing an alternating stacking of O and Zn ionic planes along the c axis. Each repeat unit (double layer) has a dipole moment perpendicular to the surface and, hence, the electrostatic potential increases monotonically as a function of crystal thickness, giving rise to a surface instability. Cutting a ZnO crystal perpendicular to the c axis creates a Zn-terminated (0001) surface on one side and an O-terminated (000 $\bar{1}$) surface on the other side. However, the macroscopic component of the dipole moment can be canceled by a modification of the charge density in the outer surface layers. In the case of ZnO, a deficiency of 25% of positive (Zn-terminated face) or negative charges (O-terminated face) induces a counterfield providing stable surface termination conditions.⁶

The stabilization mechanism for the Zn-terminated face of ZnO [Zn-ZnO(0001)] has been experimentally investigated by a variety of techniques like scanning tunneling microscopy (STM),⁸⁻¹¹ low-energy electron deflection,^{10,12,13} surface x-ray diffraction,¹⁴ and He atom scattering (HAS).^{12,13,15} Three mechanisms have been proposed for the reduction of the surface charge density to yield a stable Zn termination. One of them addressed the creation of a surface state by charge transfer of negative charges from the O-terminated to the Zn-terminated face,^{14,16} however, more recent studies indicate that electron transfer is not an adequate model¹⁷ and,

up to now, photoemission experiments could not provide evidence for the proposed surface state.^{18,19} There is an ongoing discussion as to whether a reconstruction (comprising a change in surface stoichiometry) or adsorbates stabilize the polar faces of ZnO.² Recent STM studies^{8,10} combined with *ab initio* density functional theory (DFT) calculations^{9,20} suggest that the Zn-terminated surface can be stabilized by a reconstruction involving triangular surface structures. This mechanism has been proposed to be active over a large parameter space in a phase diagram defined by oxygen and hydrogen chemical potentials. However, the associated reconstruction could not be revealed at the atomic scale. On the other hand, HAS experiments performed on the hydrogen-exposed Zn-ZnO(0001) surface reveal a stabilization by the formation of a well-ordered H-(1 \times 1) overlayer under conditions of a high hydrogen chemical potential.^{12,15}

Our investigations based on atomic scale imaging yield strong evidence that the stabilization-induced morphology of the Zn-ZnO(0001) surface is influenced by the preparation temperature. While triangular reconstructions without any apparent ordering among themselves stabilize the mildly annealed surface, upon high-temperature preparation a stabilization by a complex combination of faceting and triangular reconstruction appears, yielding highly ordered step arrays. The uniform terrace width in highly ordered faceted domains points toward a repulsive electrostatic step-step interaction. We find that step edges on Zn-ZnO(0001) exhibit exclusively $\{10\bar{1}0\}$ nanofacets, underlining the general notion that the step formation energy on metal oxides scales with the surface energy of the extended facet, emphasizing the general applicability of this concept for step edge formation on metal oxide surfaces.^{21,22}

Experiments are carried out in an ultrahigh vacuum system with a base pressure better than 10^{-10} mbar at room temperature with a commercial dynamic scanning force microscope²³ (SFM) operated in the so-called non-contact mode (NC-AFM). We use p -doped silicon cantilevers, having a resonance frequency of 75 kHz (Nanosensors) as force sensors. Our setup is operated in the constant detuning scanning mode; however, due to intrinsic loop limitations there is always a residual Δf signal containing useful information. The cantilever oscillation amplitude is kept constant and the best images were taken at an average detuning of the resonance frequency of typically -20 Hz, whereas the electro-

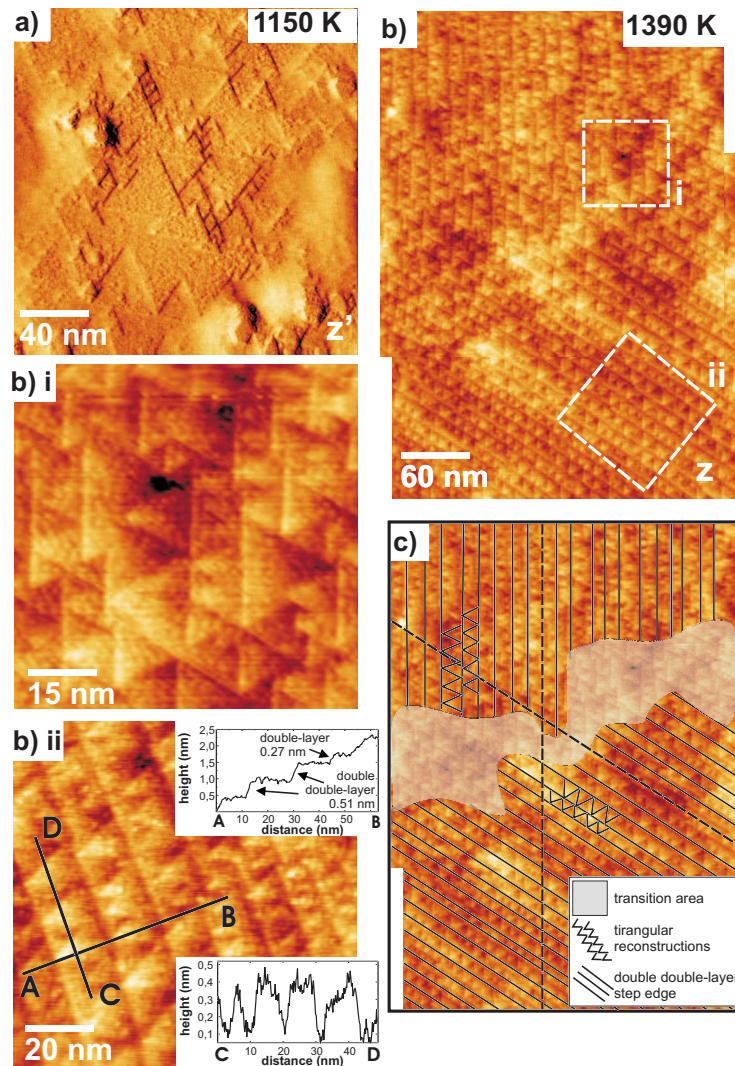


FIG. 1. (Color online) (a) Typical large-scale SFM images of the Zn-ZnO(0001) surface at an annealing temperature of 1150 K exhibit triangular shaped terraces and holes. z' denotes the spatial derivative in the fast scanning direction (horizontal). (b) Large-scale image of a Zn-ZnO(0001) surface prepared at an annealing temperature of 1390 K. (b) is assembled of two frames. (c) Schematic illustration of (b) highlighting the domain structure. (b) i and (b) ii: Zoom into the area marked by the dashed squares in (b). Cross sections taken along and perpendicular to straight step edges.

static interaction was minimized by applying a sample bias voltage of typically -0.45 V.²³ The ZnO samples (MTI Corporation) are of the highest available quality, epipolished, and oriented to within 0.2° of the c axis. The surface preparation consists of several cycles of Ar^+ -ion sputtering (1.5 keV, 5 min) and subsequent annealing for 10–15 min between 1000 and 1400 K.

Typical SFM images of Zn-ZnO(0001) surfaces taken directly after preparation at an annealing temperature of 1150 K are shown in Fig. 1(a). All terraces and islands have a triangular shape with a typical step height of 0.26 nm, representing one double layer of Zn and O ions, reflecting half of a unit cell. Triangular structures appear without any obvious ordering. Even though no atomic resolution could be obtained in previously reported STM measurements, combined DFT calculations clarified that triangular reconstructions cancel the polarity of the surface, providing a stable termination of the Zn-ZnO(0001) surface.^{9,20}

In our experiments, we systematically varied the annealing temperature to study its influence on surface morphology. When annealing at high temperature, we observe a reconstructed phase where triangles appear in ordered arrays along parallel steps. Similar structures have been observed earlier on smaller length scales; however, they were assigned to residual sputter damage¹¹ or a miscut of the surface.¹⁰ Figure 1(b) displays a typical result for a surface prepared at 1390 K. This image presents a surface that is highly faceted and exhibits two homogeneous domains of parallel terraces covered by triangular islands. Step edges alternate between a sawtoothlike and a straight morphology and form a highly regular step array spanning over several 100 nm. The distance between straight step edges varies between 8 and 9 nm. The major structural elements are illustrated by the schematic drawing in Fig. 1(c) where straight step edges are marked by solid lines. The gray shaded area highlights a region where no distinct straight step edges can be identified.

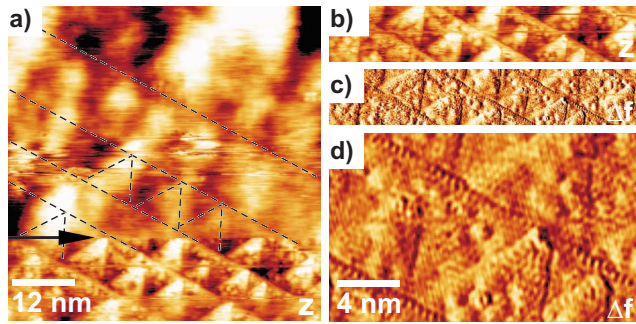


FIG. 2. (Color online) (a) Dramatic change in contrast formation due to a tip change (marked by an arrow) observed in a high-resolution image of the Zn-ZnO(0001) surface. The dashed lines highlight double double-layer step edges and triangular islands. The topography (b) as well as the detuning signal Δf (c) show atomically resolved terraces and step edges. (d) Slightly Fourier-filtered image enhancing the atomically resolved structure of triangles and step edges in detail.

This is a transition region between domains having different preferential directions for straight step edges. The zoom into the transition area shown in Fig. 1(b)i clearly demonstrates that here just regular stacking of triangular shaped islands occurs, similar to the surface structure of the mildly annealed sample shown in Fig. 1(a). When tracing straight step edges from one domain to the other, it is found that their direction is parallel to the edges of the triangular islands on the other terraces as indicated by the two dashed lines crossing the transition area. The angle between the two preferential directions is 120° , reflecting the hexagonal symmetry of the ZnO wurtzite structure. A more detailed view on a reconstructed and locally faceted domain is shown in Fig. 1(b)ii. All straight step edges are aligned parallel to each other (the slight curvature of the step edges is due to thermal drift). A cross-sectional analysis yields a step height between two straight edges of 0.51 nm, corresponding to a double double-layer (with a stacking of Zn-O-Zn-O layers) step height of one unit cell that is 0.53 nm for the ZnO wurtzite structure. Terraces are covered by triangular islands having the double-layer step height of 0.27 nm.

Zooming into the structure and decreasing the tip-sample distance to obtain higher resolution, the terraces normally appear to be rough and covered with blurry protruding features. Results shown in Fig. 2 demonstrate that the surface is not contaminated, but the limited resolution is caused by peculiarities in the tip-surface interaction that may be altered by a change in the atomic structure of the tip apex. Figure 2(a) exhibits a dramatic change in SFM contrast formation. This image has been recorded from top to bottom, and initially the contrast is rather faint and blurry. However, a critical tip change occurs at the position marked by the arrow, where possibly an O atom from a step edge has jumped to the tip. With such a tip termination the Zn sublattice would be imaged as bright protrusions. This kind of tip conditioning results in a stunningly clear contrast, providing atomic resolution that disappears after another tip change. The strong resolution enhancement allows a direct view of the atomic arrangements forming the reconstructed surface where the

basic structural elements are again straight step edges and triangles. The raw data of topography and detuning signals of the stripe where atomic resolution could be obtained are presented in Figs. 2(b) and 2(c), respectively. In Fig. 2(d) a slightly Fourier-filtered section (cutoff of high frequency noise) of Fig. 2(c) is presented to highlight the detailed atomic structure. Atomic resolution imaging on triangles and at step edges reveals a hexagonal periodicity of 0.3 nm, corresponding to the distance between next neighbors of the Zn-ZnO(0001) unit cell (0.325 nm). Atomic resolution is present over large areas on terraces and clearly at step edges, while only very few contaminants can be spotted. Typical preparation conditions during our experiments of $T > 800$ K and $p < 10^{-10}$ mbar correspond to chemical potentials of $\mu_{\text{O}} < -1.9$ eV and $\mu_{\text{H}} < -1.55$ eV (Refs. 20 and 24) for oxygen and hydrogen in reference to the phase diagram for the Zn-ZnO(0001) surface in equilibrium with H and O particle reservoirs.²⁰ Thus, our preparation conditions can clearly be associated with the regime of triangular reconstruction, in accordance with our experimental findings. Moreover, by adjusting the temperature we can control the surface morphology, switching between unordered triangular reconstructions at moderate temperatures⁹ [Fig. 1(a)] and highly ordered step arrays decorated with triangular adislands [Fig. 1(b)]. While our results fully corroborate earlier findings on triangular reconstruction on Zn-ZnO(0001), Figs. 1(b) and 2 reveal an additional aspect of the stabilization mechanism on the polar Zn-ZnO(0001) surface. Our results clearly demonstrate that the surface tends to form facets and large domains of highly regular step arrays when annealed at temperatures above 1150 K. For this phase, terraces are covered by triangular islands generating a characteristic sawtooth pattern. In the more general context of the formation of step structures on metal oxide surfaces, our study reveals a new mechanism of step edge formation and step-step interaction on metal oxide surfaces.

In the following, we discuss the origin for the regularly stepped Zn-ZnO(0001) surface. With respect to the thermodynamic stability and crystallographic structure of ZnO it should be energetically favorable to exhibit double double-layer steps, since the stacking implies that equal Zn ions repeat every third Zn layer. Our model of alternating straight and sawtoothlike step edges is outlined in Fig. 3. The model was constructed by following a concept where structures with more highly coordinated atoms are energetically more stable resulting in oxygen-terminated step edges.^{10,20} The top view of this structure shown in Fig. 3(b) reveals that straight step edges and triangular reconstructions are oriented perpendicular to the $[10\bar{1}0]$, $[\bar{1}100]$, and $[0\bar{1}10]$ directions exhibiting equivalent nanofacets, which correspond to the ZnO(10 $\bar{1}0$) surface termination. The step terminations of the three equivalent nanofacets (marked by a triangle) are displayed in Fig. 3(c). The formation of a domainlike arrangement of regular step arrays reflects the threefold surface symmetry of the wurtzite structure. Two of these respective directions are clearly seen in Fig. 1(b). This arrangement apparently lowers the surface energy and, therefore, contributes to the overall stabilization. Annealing at higher temperature and prolonged annealing cycles result in a faceted sur-

face but also facilitate the mass transport needed to modify surface stoichiometry involving the rearrangement in the surface structure for polarity cancellation. In the course of this process, ZnO units on the surface are mobile and the step edges arrange in equally spaced terraces, minimizing the electrostatic repulsion of straight step edges. Furthermore, mobile ZnO units attach at double double-layer step edges, creating the observed sawtooth features. The triangular features facilitate the necessary Zn deficiency of 25% due to the oxygen termination of step edges and only step edges of one type are formed [Fig. 3(c)]. It has been demonstrated that a dipole moment is connected to these step edges, resulting in a net electric field. The net electric field at step edges is believed to compensate the macroscopic electric field responsible for the instability of the polar surface.^{9,20} It is well known that dipole moments connected to step edges are the driving force for the formation of regular stepped metal surfaces.^{25,26} Therefore, we expect similar mechanisms to be at work on the Zn-ZnO(0001) surface, inducing highly ordered and equally spaced step edges due to a repulsive dipole-dipole interaction between straight step edges.

A literature survey⁸ yields that for standard chemical environments the ZnO($10\bar{1}0$) surface is more stable than the ZnO(0001) surface. With respect to the surface energies of the $\{10\bar{1}0\}$ planes, we understand that the formation of the $\{10\bar{1}0\}$ nanofacets at step edges—straight and sawtoothlike—contribute to the surface stabilization. A similar mechanism has already been discussed and theoretically verified for the polar SrTiO₃(110) surface.²⁷ In this study it has been demonstrated that the polarity compensation can be obtained by the formation of nanofacets, which themselves reflect stable surface orientations. Furthermore, the study demonstrates that faceting is driven by electrostatics to com-

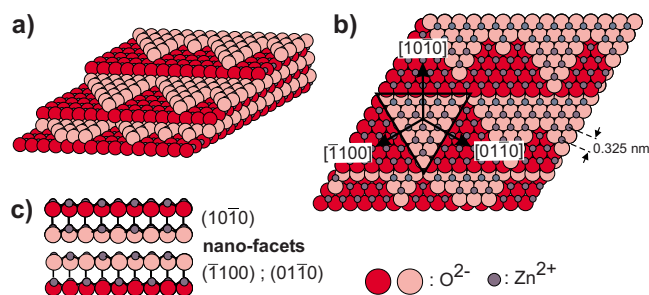


FIG. 3. (Color online) Model of the alternating straight and sawtooth step edges on Zn-ZnO(0001) as observed in Figs. 1(b) and 2. (a) Perspective view. (b) Top view. (c) Side view of the three step edges marked by the triangle in (b).

pensate polarity and by thermodynamics to lower the surface energy.

There is a lack of basic understanding of step structures on metal oxide surfaces.²² We find that step edges on Zn-ZnO(0001) exhibit exclusively the thermodynamically most stable $\{10\bar{1}0\}$ facets, underlining a general notion that the step formation energy on metal oxides scales with the surface energy of the extended facet. Therefore our results emphasize a general applicability of this concept for step edge formation on metal oxide surfaces.^{21,22} Finally, for an application like the very sintering-sensitive methanol or water-gas shift catalyst, a highly regular faceted Zn-ZnO(0001) surface might be the perfect material.

Financial support from the Deutsche Forschungsgemeinschaft is gratefully acknowledged. We are indebted to S. Gritschneider, G. Kresse, J. Lauritsen, and M. Neumann for most stimulating discussions and experimental assistance.

*reichling@uos.de

¹V. E. Henrich and P. A. Cox, *The Surface Science of Metal Oxides* (Cambridge University Press, Cambridge, U.K., 1996).

²C. Wöll, *Prog. Surf. Sci.* **82**, 55 (2007).

³C. T. Campbell, *Surf. Sci. Rep.* **27**, 3 (1997).

⁴U. Heiz and U. Landmann, *Nanocatalysis* (Springer, Berlin, 2007).

⁵P. W. Tasker, *J. Phys. C* **12**, 4977 (1979).

⁶C. Noguera, *J. Phys.: Condens. Matter* **12**, R367 (2000).

⁷R. W. Nosker, P. Mark, and J. D. Levine, *Surf. Sci.* **19**, 291 (1970).

⁸U. Diebold, L. V. Koplitz, and O. Dulub, *Appl. Surf. Sci.* **237**, 336 (2004).

⁹O. Dulub, U. Diebold, and G. Kresse, *Phys. Rev. Lett.* **90**, 016102 (2003).

¹⁰O. Dulub, L. A. Boatner, and U. Diebold, *Surf. Sci.* **519**, 201 (2002).

¹¹T. M. Parker, N. G. Condon, R. Lindsay, F. M. Leibsle, and G. Thornton, *Surf. Sci.* **415**, L1046 (1998).

¹²T. Becker, S. Hovel, M. Kunat, C. Boas, U. Burghaus, and C. Wöll, *Surf. Sci.* **486**, L502 (2001).

¹³M. Kunat, S. G. Girol, T. Becker, U. Burghaus, and C. Wöll, *Phys. Rev. B* **66**, 081402(R) (2002).

¹⁴A. Wander, F. Schedin, P. Steadman, A. Norris, R. McGrath, T. S. Turner, G. Thornton, and N. M. Harrison, *Phys. Rev. Lett.* **86**, 3811 (2001).

¹⁵C. Wöll, *J. Phys.: Condens. Matter* **16**, S2981 (2004).

¹⁶J. M. Carlsson, *Comput. Mater. Sci.* **22**, 24 (2001).

¹⁷B. Meyer and D. Marx, *Phys. Rev. B* **67**, 035403 (2003).

¹⁸R. T. Girard, O. Tjernberg, G. Chiaia, S. Soderholm, U. O. Karlsson, C. Wigren, H. Nylen, and I. Lindau, *Surf. Sci.* **373**, 409 (1997).

¹⁹W. Göpel, J. Pollmann, I. Ivanov, and B. Reihl, *Phys. Rev. B* **26**, 3144 (1982).

²⁰G. Kresse, O. Dulub, and U. Diebold, *Phys. Rev. B* **68**, 245409 (2003).

²¹X. Q. Gong, A. Selloni, M. Batzill, and U. Diebold, *Nat. Mater.* **5**, 665 (2006).

²²V. E. Henrich and S. K. Shaikhutdinov, *Surf. Sci.* **574**, 306 (2005).

²³S. Gritschneider and M. Reichling, *Nanotechnology* **18**, 044024 (2007).

²⁴K. Reuter and M. Scheffler, *Phys. Rev. B* **65**, 035406(R) (2001).

²⁵E. D. Williams, *Surf. Sci.* **300**, 502 (1994).

²⁶M. Giesen, *Prog. Surf. Sci.* **68**, 1 (2001).

²⁷F. Bottin, F. Finocchi, and C. Noguera, *Surf. Sci.* **574**, 65 (2005).